Influence of the Stacking Sequence on the Porosity in Carbon Fiber Composites

C. Toscano, C. Vitiello

Italian Aerospace Research Centre (CIRA) via Maiorise s/n, 80143 Capua (Caserta), Italy

Received 28 April 2011; accepted 28 April 2011
DOI 10.1002/app.34769
Published online 10 August 2011 in Wiley Online Library (wileyonlinelibrary.com).

ABSTRACT: Several composite laminate structures with different stacking sequences were manufactured to study how the special orientation of the fibers can influence the porosity distribution in the material. Different amounts of porosity were introduced into the laminate during autoclave curing through the application of pressures that differed from the prescribed one. All of the obtained structures were analyzed by ultrasonic inspection to measure the attenuation undergone by the signal through crossing within the material. Subsequently, the attenuation variations were associated with the induced porosity. The obtained results were corroborated by an estimation of the percentage of porosity introduced into the composites structures through the application of a standard method for density measurement. The results prove that there are stacking sequences much more subject to trap air with the consequent formation of the porosity. © 2011 Wiley Periodicals, Inc. J Appl Polym Sci 122: 3583–3589, 2011

Key words: composites; fibers; curing of polymers

INTRODUCTION

Hand layup is a typical manufacturing technique for the production of carbon fiber reinforced polymer (CFRP) composites for aircraft applications. Prepreg laminas are cut and superimposed in accordance with the established stacking sequences and thickness; then, the obtained structures are put into vacuum bags and cured in an autoclave. The curing process is achieved by the application of defined temperature and pressure cycles to get a compact structure with the expected mechanical properties. Generally, the temperature–pressure curve cycle is prescribed by the materials provider to get the optimum final components, and therefore, as a consequence, the application of a different cycle,[1] as in the case of this work, with a different pressure could be responsible for the introduction or the entrapment of air bubbles. Trapped air in a composite structure is responsible for porosity formation[2,3] or, in the worst case, for local debonding of the laminas. It has been proven that this kind of defect can strongly reduce the mechanical properties of the components,[4] with the consequent danger of their disruption during the in-service life. That makes evident why the detection of defects arising from the manufacturing process is a fundamental means for avoiding future damages of the structures and, as well, for optimizing the manufacturing process. In this context, it is interesting to look for the structures that are more exposed to the porosity formation.

In this study, several hand layup coupons were manufactured with different stacking sequences and with induced porosity. The induced porosity was produced by the application of five different pressures during autoclave curing. The presence of the porosity was detected and evaluated by means of ultrasonic testing (UT).[5] The obtained results were corroborated by the results found through the application of a standard method for density measurement, which led to the estimation of the percentage of entrapped air in the tested structures. The obtained results allowed us to demonstrate the influence of the stacking sequence on the rate of porosity formation.

EXPERIMENTAL

In the following paragraphs, the tested specimens and the used inspection technique are described. In particular, the inspection of the specimens was achieved through a nondestructive evaluation methodology, UT, and by means of a destructive methodology, that is, density measurement by means of a digital balance.

UT for the detection of bulk porosity

The nondestructive inspection was carried with UT in the Pulse-Echo (PE) arrangement in immersion

Correspondence to: C. Toscano (c.toscano@cira.it).

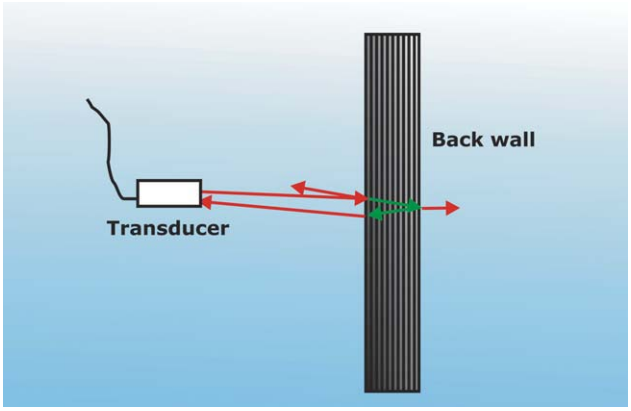

Figure 1 Typical set up for PE in immersion. [Color figure can be viewed in the online issue, which is available at wileyonlinelibrary.com.[

(Fig. 1), and the results were evaluated through the obtained c-scans.

In general, in a PE inspection, the total signal attenuation (A_T) undergone by the signal can be assumed as given by the sum of more contributions:

$$A_T = A_R + A_B \tag{1}$$

where A_R represents the losses due to the reflections of the signal at the encountered interfaces, which are water–specimen and specimen–water, and A_B is the bulk attenuation due to the double passage within the specimen. Therefore, by the measurement of the attenuation undergone by the signal coming from the back wall (Fig. 1), A_T can be obtained.

From the literature,[6] the intensity (I_0) of a propagating ultrasonic signal within a material decreases exponentially along its path. Thus

$$I(z) = I_0 e^{-\alpha z} \tag{2}$$

where z is the propagation direction of the ultrasound and α is the attenuation coefficient of the material, that is, A_B divided for the specimen thickness.

This leads to the assumption that the presence and the amount of porosity can be estimated by measurement of A_B. In fact, the presence of voids or porosity in the material under inspection has a strong influence on the attenuation of the ultrasonic signal passing through it:[7,8] the absorption and the scattering due to the air bubbles increase the attenuation within the material. Of course, this effect depends on the frequency of the ultrasonic wave, the dimensions, and the density of the air bubbles.

Taking into account the previous considerations and the convenience to inspect all of the manufactured structures with the same transducer, we used a Panametrics (Waltham, MA) flat 5-MHz probe with a diameter of 0.25 in. for all of the inspections.

Measure of the density of the materials

By a digital analytical balance, the density of the material of the coupons was measured through the application of the Archimedean principle. Knowing the density of each element of the composite structure, we could estimate the percentage of the air trapped in the material, that is, the percentage of porosity. To do that, we assumed that the fiber volume ratio and the resin volume ratio remained the same for all of the coupons, whereas the introduction of air was responsible for volume variations. The previous considerations could be translated into equations; for the theoretical density (ρ_T), we have

$$\rho_T = \frac{\rho_f V_f + \rho_r V_r}{V_f + V_r} \tag{3}$$

where ρ_f, V_f, ρ_r, and V_r are the densities and volumes of the fibers and the resin, respectively. If the volume of the vacuum (air) is introduced we have

$$\rho = \frac{\rho_f V_f + \rho_r V_r}{V_f + V_r + V_v} \tag{4}$$

where ρ is the density measured by the digital balance and V_v is the vacuum volume. Then, the total volume (V_T) = $V_f + V_r + V_v$.

If eqs. (3) and (4) are multiplied and divided for V_T, it can be obtained as follows, respectively:

$$\rho_T = \frac{\rho_f V_{f\%} + \rho_r V_{r\%}}{V_{f\%} + V_{r\%}} \tag{5}$$

$$\rho = \rho_f V_{f\%} + \rho_r V_{r\%} \tag{6}$$

where fibre-volume fraction and resin-volume fraction are respectively defined as

$$V_{f\%} = \frac{V_f}{V_T}, \qquad V_{r\%} = \frac{V_r}{V_T}$$

The ratio between the eqs. (6) and (5) is

$$\frac{\rho}{\rho_T} = V_{f\%} + V_{r\%} \tag{7}$$

From (7), it can be obtained

$$V_{r\%} = \frac{\rho}{\rho_T} - V_{f\%} \tag{8}$$

With eqs. (8) and (6), through a bit of algebra, some useful relations can be obtained:

$$V_{f\%} = \frac{\rho - \frac{\rho_r \rho}{\rho_T}}{\rho_f - \rho_r} \tag{9}$$

TABLE I
Reference Densities Used for the Calculation of the Percentage of the Void Volume

Density (g/cm^3)	
ρ_r	1.28
ρ_f	1.78
ρ_T	1.56

$$V_{V\%} = 1 - V_{f\%} - V_{r\%} \quad (10)$$

where $V_{V\%}$ is the percentage of the void volume.

Of course, the theoretical values (Table I) for ρ_f, ρ_r, and ρ_T, reported in the material datasheet, should be used for the final calculations.

Tested specimens

The specimen manufacturing was carried out with the preimpregnated laminas M21/IM7 provided by Hexcel Corporation (Stamford, CT), which were laid up by hand, sealed in a vacuum bag, and cured in an autoclave. To study the influence of the orientation of the carbon fibers on the diffusion of porosity in the laminated composites, three typical stacking sequences were taken into account, as shown in Table II.

Specimens for UT characterization of the employed structures and materials

In the first part of the study, a materials ultrasonic characterization was carried out to measure α and A_R. To do that, specimens with different thicknesses were produced for each stacking sequence. The Hexcel-recommended curing cycle was applied to cure the specimens. Then, the density of the obtained structures were measured to ensure that they were free of voids; thus, they were treated as a reference.

Specimens of type P1 and P2 were manufactured according to the geometry indicated in Figure 2. Therefore, four different thicknesses were obtained in the same laminate. The thickness of each part (A, B, C, and D in Fig. 2) was measured by a Palmer caliper.

Coupons of type P3 were manufactured according to the geometry indicated in Figure 3. In this case, two different thicknesses were obtained in the same laminate. The thicknesses of each part (A and B, Fig. 3) were measured by a Palmer caliper also.

TABLE II
Used Stacking Sequences

Type	Stacking sequence
P1	$[0°]$
P2	$[90°]$
P3	$[45°/-45°]_S$

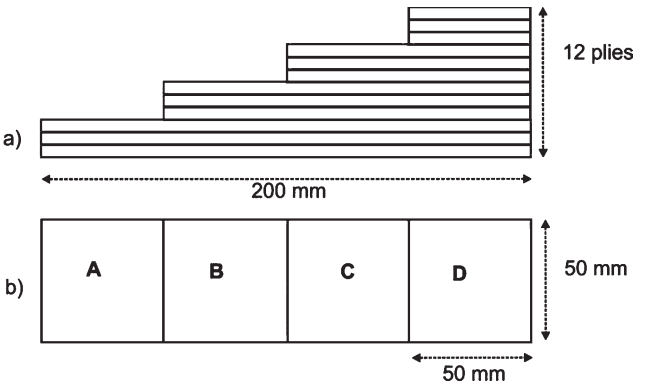

Figure 2 Geometry used for the type P1 and P2 coupons: (a) lateral view and (b) frontal view.

By UT, A_T was measured with gating on the back wall of each thickness. A distance–attenuation graph was obtained for each specimen. In this way, α resulted as the slope of the graphs, and A_R was the intercept.

Specimens with induced porosity

In the last part of this study, a new set of coupons was produced with the three stacking sequences. To obtain structures with induced porosity with the chosen manufacturing process (hand layup), two parameters were the main actors: the pressure and the temperatures used during the autoclave curing. The applied pressure could principally influence the kinetics of the resin flowing in the vacuum bag,

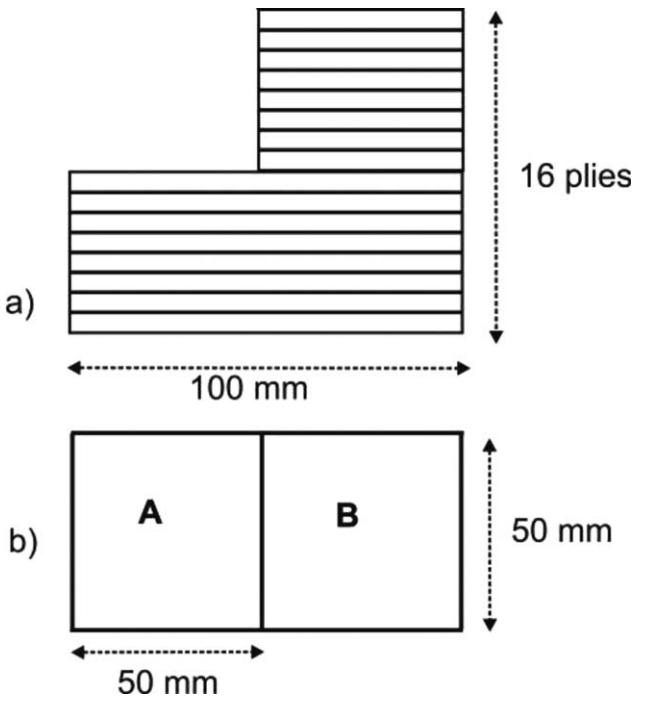

Figure 3 Geometry for the type P3 coupons: (a) lateral view and (b) frontal view.

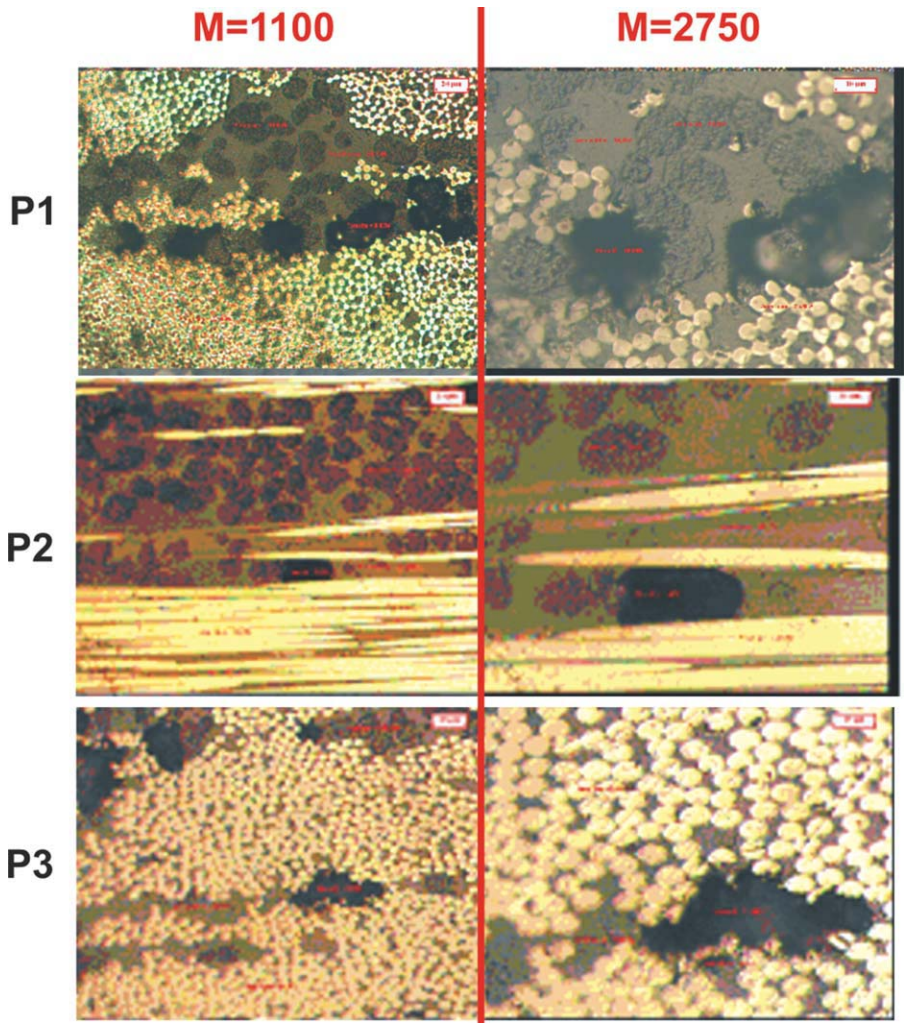

Figure 4 Images obtained by optical microscopy with two different magnification factors: 1100 and 2750×. The images were taken from the three types of specimens cured with the 0% of the pressure; the presence of porosity could be appreciated. [Color figure can be viewed in the online issue, which is available at wileyonlinelibrary.com.]

whereas the temperature was responsible for the appropriate viscosity of the resin, which had to bond the laminas and impregnate the fibers. Thus, a change in the cited parameters in the prescribed curing cycle was undoubtedly responsible for the introduction of defects in the obtained structure. In this work, to introduce a controlled porosity in the structures, we chose to apply only a fraction of the prescribed pressure (7 bar) during the autoclave curing.

TABLE III
Schematic of the Manufactured Coupons

		No. of coupons cured at different pressures				
Stacking sequence	No. of plies	100%	75%	50%	25%	0%
P1: 0°	24	3	3	3	3	3
P2: 90°	24	3	3	3	3	3
P3: $[(45°/-45°)_6]_S$	24	3	3	3	3	3

As an example of the introduced porosity, in Figure 4, some optical microscopy images are shown for the three types of specimen cured with 0% of the pressure. In Table III, the used stacking sequences,

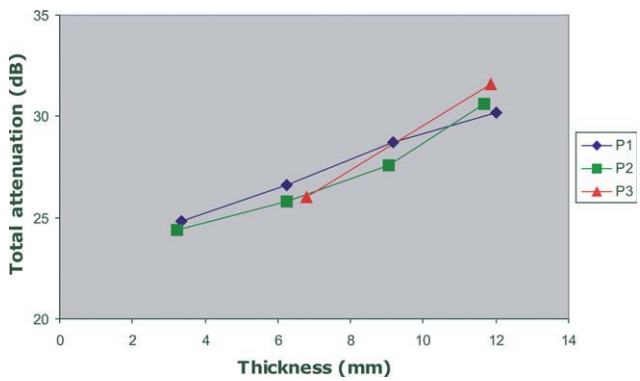

Figure 5 Distance–attenuation graph. [Color figure can be viewed in the online issue, which is available at wileyonlinelibrary.com.]

TABLE IV
Results Obtained for the Slope and Intercept of the Distance–Attenuations Graphs

Type	α (dB/mm)	A_R (dB)
P1	0.63	22.71
P2	0.72	21.65
P3	1.11	18.47

the number of plies, the applied pressures (as percentages of the prescribed one), and the number of produced coupons are reported. All of the coupons had a rectangular shape with dimensions of 100 × 50 mm^2.

The coupons were shared in sets of four types, and each set was processed by a dedicated autoclave curing at the established pressure.

All of the coupons in Table III were inspected by UT to measure A_T to obtain A_B. A_T was obtained by the averaging of thousands of points of the back-wall c-scans, with care taken to avoid the edges. A_B was used to calculate α, which was directly related to the amount of porosity within the specimen.

With A_R assumed to be the same measured for the reference coupons (as described earlier), we calculated α, starting from the measured A_T and the specimen thickness, as follows:

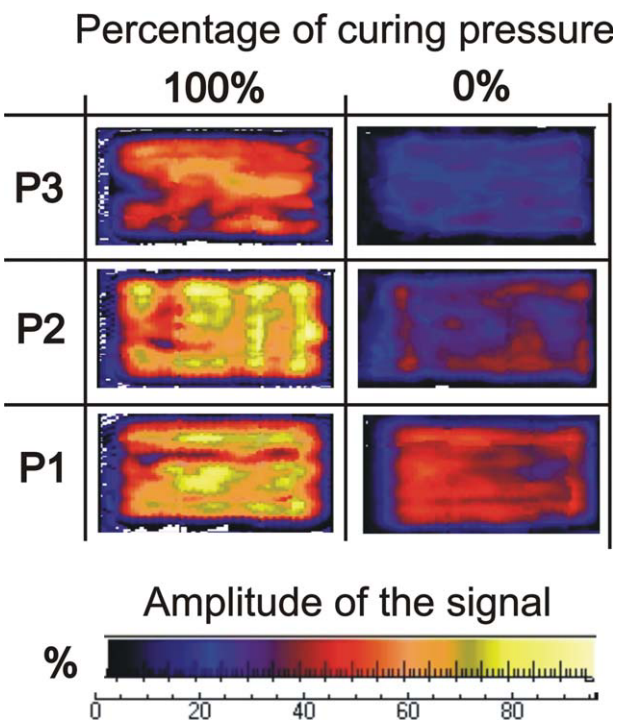

Figure 6 Example of the amplitude c-scans of the three specimen types obtained for 100% and 0% of the curing pressure. The amplitude of the signal is represented with a false color scale, and it is expressed as a percentage of the full scale. [Color figure can be viewed in the online issue, which is available at wileyonlinelibrary.com.]

TABLE V
Normalized α Values of the Coupons with Induced Porosity

	α (dB/mm)		
Pressure (%)	P1	P2	P3
100	1.00	1.00	1.00
75	0.97	0.99	1.06
50	1.07	1.18	1.11
25	1.04	1.17	1.21
0	1.33	1.34	1.47

$$\alpha = \frac{A_B}{2 \times \text{Thickness}} = \frac{A_T - A_R}{2 \times \text{Thickness}} \quad (11)$$

The previous assumption about A_R was equivalent to neglecting the influence of the external lamina porosity on the losses due to the reflection at the water–specimen interface.

RESULTS

Reference specimens: Surfaces losses and attenuation coefficient

In Figure 5, the distance–attenuation graph is shown for each specimen (the thicknesses reported in the graphs are twice the real thicknesses because of the double passage of the signal within the material). In Table IV, the results obtained for α and A_R are reported.

Results for the coupons with induced porosity

By PE, the A_T values were measured on the signal reflected by the back wall. In Figure 6 are shown, as an example, the c-scans obtained for the type P3 specimen in the case of 100 and 0% of the curing pressure, where the variation of the amplitude of the signal (expressed as percentages of the full scale) could be appreciated.

A_T, expressed in decibels, was measured by the averaging of thousands of points, with care taken to

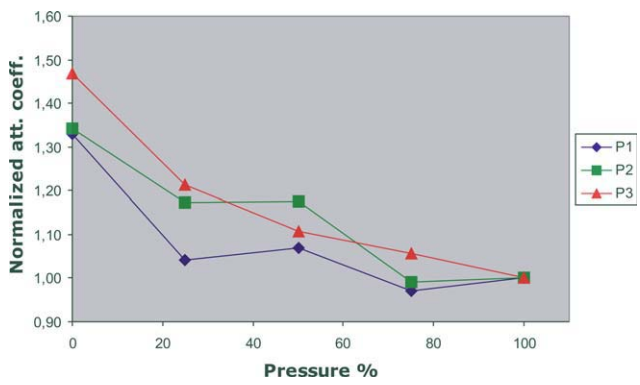

Figure 7 Trends of α versus the pressure as a percentage of the prescribed one. [Color figure can be viewed in the online issue, which is available at wileyonlinelibrary.com.]

TABLE VI
Rate of Porosity Formation versus Decreasing Pressure

	P1	P2	P3
Slope	0.0029	0.0035	0.0044

exclude the edges of the specimen. To highlight the effect of the induced porosity, A_R was subtracted from A_T. The obtained values were divided by the double of the thickness to eliminate the effect of the path length. The resulted attenuation, normalized with respect to the references values obtained for the coupons cured at 100% of the pressure, are reported in Table V.

In Figure 7, the behavior of the normalized α versus the applied curing pressure are shown for each stacking sequence. The variation of α was a function of the density of the induced porosity; all of the trends were descending with increasing pressure, as expected. Coupon type P3 behavior was exponential-like, whereas the P1 and P2 trends were more oscillating. If the previous trends were supposed to be roughly linear, the absolute value of the slope of the curves (Table VI) was the rate of porosity formation as a function of the decreasing applied pressure.

As a result, the stacking sequence P3 was the most sensitive to pressure variations.

Density measurement by the digital balance

From each coupon, a set of three samples was cut, and its density was measured by a digital balance by means of the Archimedean principle. Then, the percentage of the voids in the materials was calculated with eqs. (8)–(10) and the data of Table I.

The resulting percentages of trapped air (normalized with respect to the reference values obtained for the coupons cured at 100% of the pressure) in each coupon type are reported in Table VII, and in Figure 8, their behavior with respect to the increasing pressure is shown.

In this case, the P2 and the P3 rate of air entrapment due to the decreasing pressure are higher

TABLE VII
Percentage of Air/Voids Embodied in the Coupons

	Percentage of air		
Pressure (%)	P1	P2	P3
100	0.68	0.98	0.99
75	2.78	3.00	2.90
50	3.46	3.78	3.92
25	5.45	6.67	5.60
0	5.76	7.06	7.24

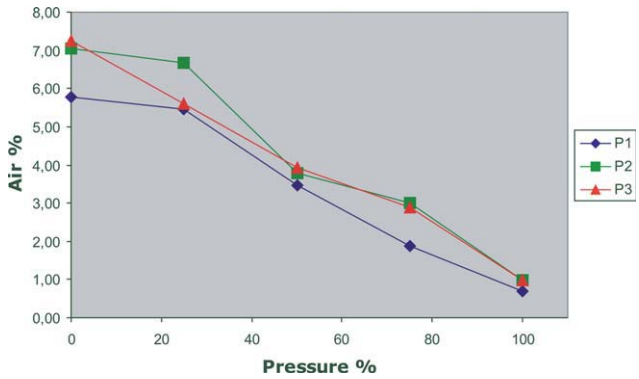

Figure 8 Percentage of the entrapped air versus the pressure. [Color figure can be viewed in the online issue, which is available at wileyonlinelibrary.com.]

(in absolute value) than the P1 rate, as shown in Table VIII.

Being the air entrapment the principal responsible of the ultrasonic attenuation increasing, in the Figure 9, the previously obtained attenuation coefficients are represented as function of the measure percentage of the air.

Because of the 1 : 1 correspondence between the percentage of the air measured by density estimations and the decreasing pressure, the exponential-like dependence of α versus decreasing pressure is still found, as well as the oscillating behavior for the P1 and P2 coupon types.

CONCLUSIONS

To highlight the dependence of the porosity formation to the selected stacking sequence of hand layup composite structures, a set of coupons with three different stacking sequences and induced porosities were prepared. The induced porosity was achieved during the curing cycle by the application of a fraction of the recommended pressure. This procedure could be assumed as a simulation of an incorrect applied curing cycle. Thus, the effect of this manufacturing process on the quality of the final component was studied. The induced porosity was first evaluated by the application of the ultrasonic inspection, with all of the contributions to the attenuation undergone by the ultrasonic signal taken into account. Then, A_B per unit length, that is, α, was measured for each coupon. In this way, a correspondence between the amount of introduced porosity and the stacking sequence was found, and in

TABLE VIII
Rate of Air Entrapment versus Decreasing Pressure

	P1	P2	P3
Slope	0.005	0.006	0.006

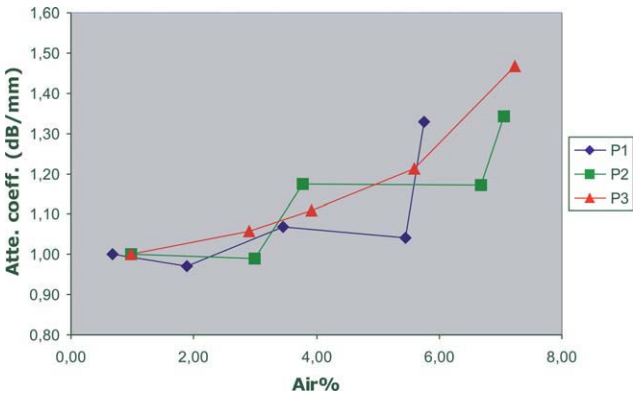

Figure 9 Normalized α behavior versus percentage of the air. [Color figure can be viewed in the online issue, which is available at wileyonlinelibrary.com.]

particular, by ultrasonic measurements, we demonstrated that the specimens with a [±45°] orientation of the fiber were more sensitive to porosity formation. The results obtained for the three types of specimens were corroborated by the results found by a standard density measuring method. The small discrepancies between the results obtained for the P3 type by the ultrasonic method and the density measure method could be ascribed to the different approaches: in the first case, the method involved as much as possible the whole specimen; on the contrary, in the second case, only the selected samples were measured. Therefore, they were probably too small to contain enough information.

References

1. Liu, L.; Zhang, B. M.; Wang, D. F.; Wu, Z. J. Compos Struct 2006, 73, 303.
2. Tang, J. M.; Lee, W. I.; Springer G. S. J. Compos Mater 1987, 21, 421.
3. Browning, C. E.; Campbell, F. C.; Mallow A. R. J. Adv Mater 1995, 26, 18.
4. Yoshida, H. T.; Ogasa, T.; Hayashi R. Compos Sci Technol 1986, 25, 3.
5. Rubin, M.; Jerina K. L. Compos Eng 1993, 3, 601.
6. Ktrautkrämer, J.; Ktrautkrämer, H. Ultrasonic Testing of Materials, 4th ed.; Springer-Verlag: Heidelberg, Germany, 1990.
7. Jeong, H.; Hsu D. K. Ultrasonics 1995, 33, 3,19.
8. Stone, D. E. W.; Clarke B. Non-Destructive Test 1975, 8(3),137.